ELSEVIER

Diamond and Related Materials 10 (2001) 1868–1874

DIAMOND AND RELATED MATERIALS

www.elsevier.com/locate/diamond

The introducing of fluorine into the deposition of BN: a successful method to obtain high-quality, thick cBN films with low residual stress

Seiichiro Matsumoto*, W.J. Zhang[1]

Advanced Materials Laboratory, National Institute for Materials Science, 1-1 Namiki, Tsukuba-city 305-0044, Japan

Abstract

Cubic boron nitride films were synthesized on silicon substrates by DC-bias-assisted DC jet chemical vapor deposition in an $Ar–N_2–BF_3–H_2$ system. By this method, the deposition of cBN at high gas pressure of 50 torr became possible, and the conditions of cBN CVD approached to those of diamond CVD. cBN films with low residual stress (1–2 GPa) and with large crystal size of up to several hundred nanometers were obtained and clear Raman peaks of cBN appeared. Furthermore, the deposition rate was as high as 0.3 μm/min at the initial stage and over 20-μm-thick BN films were obtained for a 3-h deposition. These remarkable improvements are attributed to the preferential etching effect of fluorine to sp^2 bonds and the decrease of the bombarding energy of ions.

Keywords: Cubic boron nitride; Chemical vapor deposition; Fluorine; Stress; Raman spectra

1. Introduction

Due to its unique properties, i.e. its hardness being second only to diamond, high thermal conductivity, chemical inertness, and wide band gap in connection with p- and n-type dopability, cubic boron nitride (cBN) is a highly promising material for optical, electronic and mechanical applications. During recent years, much effort has been put into improving the quality of cBN films, and different kinds of deposition methods, including both physical vapor deposition (PVD) [1–6] and chemical vapor deposition (CVD) [8–13] have been tried. For all these methods, energetic-particle bombardment of the substrate was found to be essential for the formation of the cubic phase of boron nitride. However, from the bombardment during film growth, the deposited cBN films generally exhibited a high compressive stress, which was believed necessary to obtain a cubic phase [14]. The high stress results in a limited maximum film thickness (several hundred nanometers) that can be deposited free from peeling.

To minimize the stress in the film, many different methods, including growth at a reduced ion energy [7], the use of a buffer layer [15], post-deposition annealing [16] and irradiation with high energy ions [17], were demonstrated to be more or less effective. However, the film thickness was still limited within 1 μm. Up to

* Corresponding author. Fax: +81-298-52-7449.
E-mail address: matsumoto.seiichiro@nims.go.jp (S. Matsumoto).
[1] Present address: Department of Physics and Material Science, City University of Hong Kong, Hong Kong.

0925-9635/01/$ - see front matter
PII: S0925-9635(01)00461-7

now, it has not been possible to prepare cBN films with high quality and sufficient thickness to be identified by Raman spectroscopy.

In contrast to the deposition of diamond films, the growth mechanism of cBN films by the currently successful deposition techniques may be dominated by physical effects at the surface or subsurface region regardless of the PVD or CVD. This difference is possibly due to the lack of an effective chemical reactant as hydrogen does in the diamond growth process by preferentially etching the sp^2 components and stabilizing the sp^3 structure. In this work, fluorine was introduced into the reactant gases, which was found to be very beneficial for the deposition of cBN films at a lower effective substrate bias; therefore, the residual stress was intensively decreased and cBN films with a thickness over 20 μm were successfully synthesized.

2. Experimental

2.1. Deposition experiments

cBN films were deposited on Si(001) substrates by DC jet chemical vapor deposition in an $Ar + N_2 + BF_3 + H_2$ gas system. A negative DC bias was applied to the substrate. Detailed setup of the deposition apparatus was reported elsewhere [18] and the deposition parameters are summarized in Table 1. The N/B ratio in the Table 1 is approximately 1000:1, which is much higher than the formerly reported value for the deposition of cBN films. Actually, we changed the N_2 flow rate in a wide range from 10 to 1500 sccm and cBN can be obtained at all these N_2 flow rates. However, the plasma was more stable at the N_2 flow rate of 1500 sccm, which favored to control and repeat the experiments.

2.2. Characterization

Film morphologies were studied by secondary electron microscopy (SEM) and the chemical composition was analyzed by electron probe micro analysis (EPMA). The phase composition and crystal structures were investigated by Fourier-transformed infrared spectroscopy (IR), Raman spectroscopy, glancing angle X-ray diffraction (XRD), electron diffraction (ED) and transmission electron microscopy (TEM). Raman spectroscopy was measured in macro and micro modes, with a spot size of 200 μm and 1 μm, respectively, by using a 514.5-nm line of an argon-ion laser with backscattering geometry. In XRD measurement, a Cu-Kα ray was used with an incident angle of 0.5° and the diffraction pattern was taken in a 2θ continuous mode.

Table 1
Process parameters for the deposition of c-BN films by DC jet plasma CVD

Gas flow rate	
Ar (slm)	20
N_2 (slm)	1.5
BF_3 (10% in Ar base) (sccm)	30
H_2 (sccm)	5
Substrate temperature (°C)	1000–1150
Pressure (torr)	50
Bias voltage (V)	85
Duration (min)	10, 60, 180

3. Results and discussion

Fig. 1 shows SEM plan and cross-sectional morphologies of cBN films deposited for different time. Film thicknesses of approximately 3, 12 and 27 μm were obtained for depositions of 10, 60 and 180 min, respectively. Fig. 2 shows BK and NK X-ray spectra by EPMA analysis of the cBN film deposited for 60 min and commercially available pyrolytic BN (pBN). The curve profiles of BK spectra coincide well with those reported for cBN and hexagonal boron nitride (hBN) [19]. From the relative intensity of BK to NK spectra for cBN and hBN, an almost identical elemental composition of B and N as that in pBN (B/N = 1:1) was revealed in the cBN film. The three samples in Fig. 1 were also investigated by glancing angle XRD, as shown in Fig. 3. It can be seen that intense and sharp peaks for cBN reflections appeared in all the three diffraction patterns. There are peaks for hBN, turbostratic boron nitride (tBN) and Si as well. The peak positions and half widths at half maximum (FWHM) of the cBN peaks are summarized in Table 2. The corresponding IR spectra of the samples are shown in Fig. 4. For the films deposited for 10 min, a strong absorption of cBN and weak absorption of hBN can be seen. Because the film is thick, interference fringes appeared in the high wave-number side. For the films deposited for 60 and 180 min, not only the cBN absorption but also the hBN absorption increased and their corresponding transmittance decreased to zero as well. In addition, an absorption in the range from 1700 to 2100 cm^{-1} was observed, which was previously observed from the cBN crystals synthesized by high pressure high temperature methods (HPHT) and was considered to be due to more complex vibration processes caused by the interaction of the photon with more than one phonon [20]. The low transmittance background of the films deposited for 60 and 180 min may be caused by the accumulation of defects, inclusion of impurities (though we have not analyzed this yet), increase of surface roughness (see

Fig. 1c,e), mixing of cBN and hBN/tBN phases, etc. A rough surface and the inclusion of other phases scatter the incident IR and decrease the transmittance. Fig. 5 is the corresponding Raman spectra of the samples. Except for a Si peak at approximately 980 cm^{-1}, three peaks are observed. Two intensive peaks are the transverse optical (TO) and longitudinal optical (LO) phonon modes of c-BN, while the weak one is due to the h-BN phonon mode ($2E_{2g}$), as marked in the figure. The peak positions and the FWHM of the TO and LO phonon peaks are summarized in Table 3. From the above measurements, we can summarize the characteristics of the cBN films deposited by the present method as follows.

(i) *High phase purity*. A cBN content over 90% was estimated from the IR spectrum for the sample deposited for 10 min (Fig. 4a and [18]). Because amorphous and hBN layers exist between the substrate and the cBN layer [21] and they contributed to the IR spectrum, phase purity at early growth stage of cBN itself must be higher then 90%. For the films deposited for 60 and 180 min, we cannot give even a rough estimation of cBN content from the IR spectra (Fig. 4b,c). However, the phase purity of cBN seems to decrease as the deposition time increases from the relative intensities of hBN and tBN in the XRD patterns in Fig. 3. Meanwhile, from the FWHM of the cBN peaks in XRD and the Raman spectra, it can be seen that crystal quality increases when the deposition time increases from 10 min to 1 h and again deteriorates for a longer deposition time of 3 h (Table 2). The deterioration of the phase purity and crystal quality at longer deposition times is either due to the reduction of DC jet power and the bias current (for example, 30% and 80% decrease of jet power and bias current, respectively, for an 180-min deposition) or due to the decrease of effective bias applied on the substrate with increasing film thickness. The decrease of the jet power was required to keep the substrate temperature constant. Otherwise, the substrate temperature becomes too high because the stress-induced bending of the substrate decreases the cooling efficiency of the substrate by the water-cooled substrate holder.

(ii) *Large crystal size*. Cross-sectional SEM images (Fig. 1) show a columnar structure of all the films, demonstrating the formation of crystalline material. By TEM observations, each column was found to be nearly a single crystal with a lateral size of 0.2–0.5 μm and the length across the film thickness [21]. However, the crystals have usually large amount of defects such as stacking faults and twins, and this must be one of the main reasons for the one-order smaller crystal size estimated by XRD (Table 3). Interestingly, although the surface of these films are composed of fine crystallite of tens of nanometers, we often observed flat

Table 2
Measured lattice spacing and FWHM of cBN reflections in Fig. 3. as compared with JCPDS data

JCPDS 35–1365			10 min		60 min		180 min	
hkl	d (Å)	I/I_0	d (Å)	FWHM (deg.)	d (Å)	FWHM (deg.)	d (Å)	FWHM (deg.)
111	2.0872	100	2.0920	0.66	2.0914	0.49	2.0922	0.57
200	1.8081	5	1.8146	0.75	1.8119	0.65	1.8126	0.62
220	1.2786	24	1.2805	0.89	1.2798	0.62	1.2801	0.78
311	1.0900	8	1.0914	1.28	1.0911	0.88	1.0912	0.99

Table 3
Peak position and FWHM of the cBN Raman peaks in Fig. 5, stress evaluated from the cBN TO mode peaks in the Raman spectra, and stress and crystal size calculated from the cBN 111 peaks in XRD

Growth time (min)	Raman spectroscopy				X-Ray diffraction	
	Mode	Peak position (cm^{-1})	FWHM (cm^{-1})	Stress (GPa)	Crystal size (Å)	Stress (GPa)
10	TO	1048.4	28.8	−1.5	180	−2.0
	LO	1301.8	19.7			
60	TO	1053.6	14.8	−1.0	270	−1.9
	LO	1304.8	10.4			
180	TO	1054.6	23.0	−1.9	200	−2.3
	LO	1303.3	17.8			

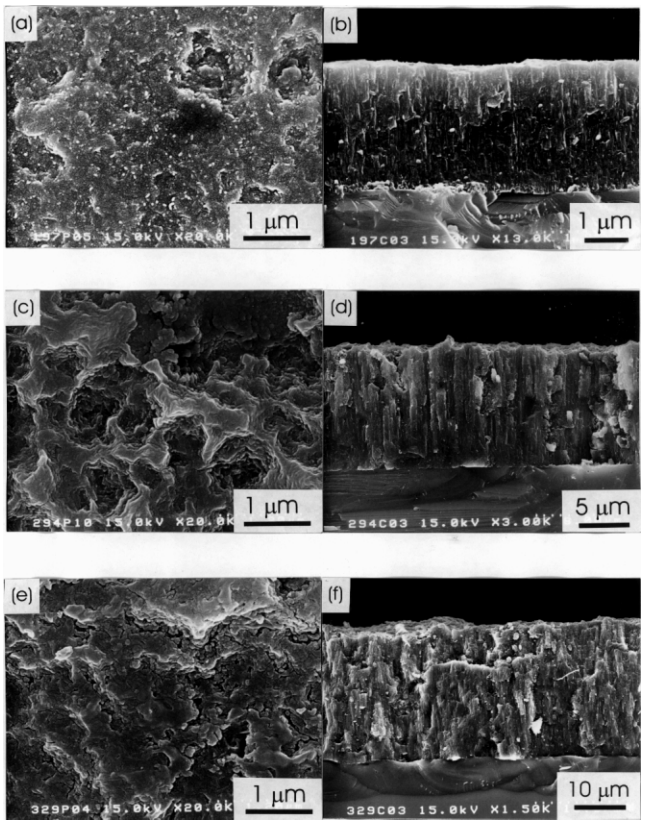

Fig. 1. SEM plan and cross-sectional images of cBN films deposited for (a, b) 10 min, (c, d) 60 min and (e, f) 180 min.

planes of submicrometer size on fractured cross sectional faces as shown in Fig. 6. Referred to the results of the TEM observations, this is probably a crystal face of cBN with low Miller indices.

(iii) *Thick films*. Over 20 μm of the film thickness was achieved for a 3-h deposition, which is much larger than the thickness limit of 1 μm so far reported. This achievement is believed to be due to the low stress in the films as will be discussed below. The deposition

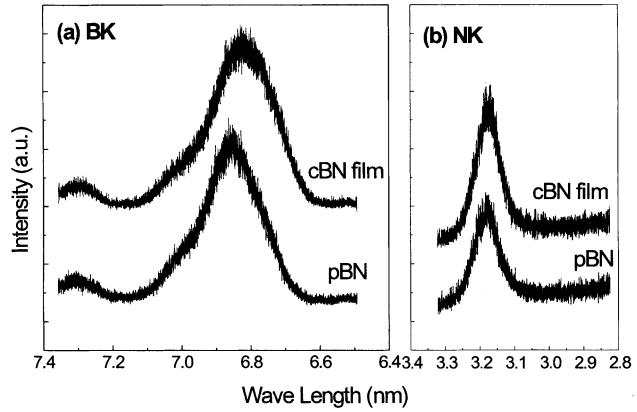

Fig. 2. Results of electron probe micro-analysis for the cBN film deposited for 60 min.

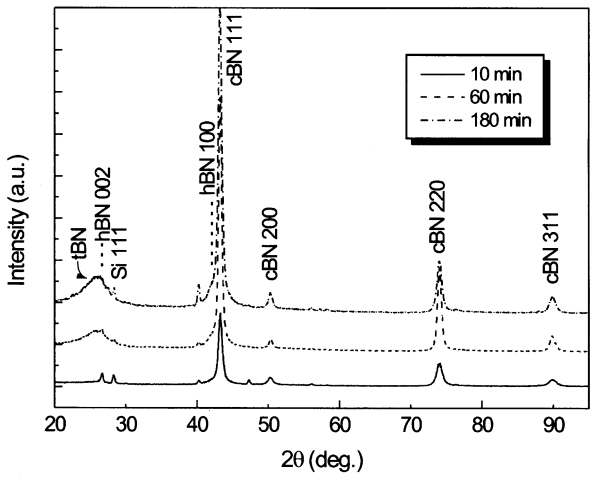

Fig. 3. Glancing-angle X-ray diffraction patterns of the cBN films deposited for 10, 60 and 180 min, respectively.

rate is fast at the early stage of growth, i.e. 0.3 μm/min for the first 10 min, which is five times higher than the maximum reported so far for cBN growth [6]. However, the growth rate decreases with the increase of film thickness because of the decreasing jet power as discussed above.

(iv) *Good adhesion to substrates and low stress*. The cBN films can be kept free from peeling over 8 months after deposition. This good adhesion can be attributed to the low stress in the films. The stress in the films was evaluated from both the peak shift of the XRD with the assumption of a biaxial stress and the peak shift and line broadening of the Raman peaks [22]. The

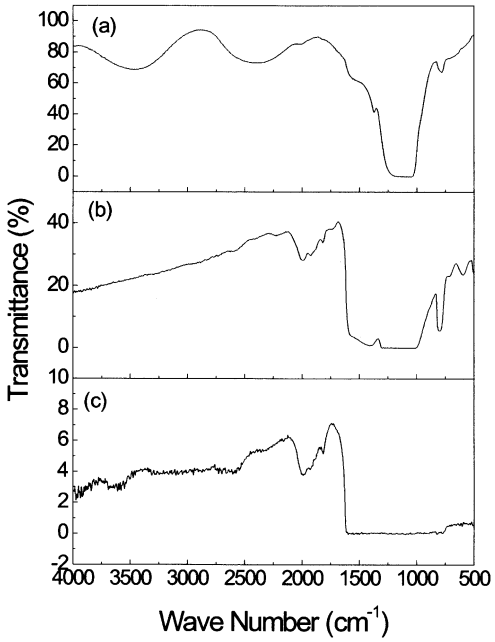

Fig. 4. IR transmission spectra of the cBN films deposited for (a) 10 min, (b) 60 min and (c) 180 min.

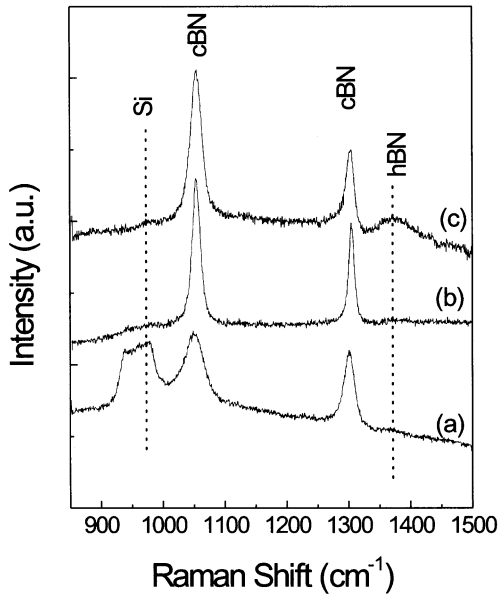

Fig. 5. Raman spectra of the cBN films deposited for (a) 10 min, (b) 60 min and (c) 180 min.

results are summarized in Table 3. The stress is 1.5–2 GPa for the 10-min film and decreases to 1–1.9 GPa for the 60-min film and again increases to 1.9–2.3 GPa for the 180-min film. This change of stress with time is in accordance with the film quality as revealed by Raman spectroscopy. The values of stress here are much lower than the values of 4–20 GPa in cBN films reported previously [23,24].

(v) *Rough surface*. In contrast to the surface of CVD diamond films, which usually show faceted crystal planes, the present cBN films have rough surfaces with many pits, and composed of fine particles (Fig. 1a,c,e). The depth of these pits increased with deposition time. These rough futures are very popular for films deposited with ion bombardment under high gas pressures [25]. However, it is amazing that in spite of these rough surfaces, the crystal size is as large as submicrometers as observed by TEM [21], the reason for which remains unclear and should be considered in relation to the growth mechanism of cBN.

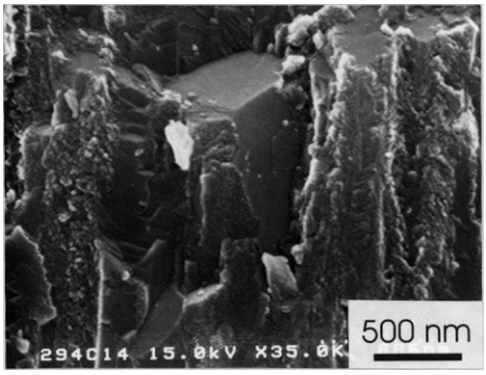

Fig. 6. Enlarged cross sectional SEM images of the fractured cBN film deposited for 60 min suggesting the appearance of flat crystal planes.

(vi) *Existence of interface layers*. A layer structure of Si/amorphous-BN/hortBN/cBN was revealed by TEM observations, as has been found in cBN films prepared by energetic ion bombardment methods. However, the intermediate layers are thicker (for example, approx. 150 nm [21]) and the hexagonal layers were not perpendicular to the substrate surface but more inclined and more randomly orientated. This is probably caused by low stress in our films, The details are discussed by Zhang and Matsumoto [21].

The following three factors are believed to be essential for the present cBN deposition method: (i) the use of fluorine-containing gas; (ii) substrate bias; and (iii) high density plasma. Fluorine is essential for the growth of cBN; when B_2H_6 or BCl_3 was used instead of BF_3 under the same conditions shown in the experimental part, only hBN but not cBN was deposited [26]. However, even with fluorine, if no substrate bias was applied, no deposition of cBN occurred, but the substrate was etched or only thin hBN films deposited [26]. This implies that ion bombardment induced by substrate bias must be indispensable for the formation of sp^3 bonds.

DC arc jets have been known to give the highest deposition rate of diamond among all the CVD methods. This high deposition rate is caused by the high density of reactive species originating from high plasma density and high gas pressure, and by the high gas flow rate to the substrate. In the deposition of cBN films, the concentration of reactive species is supposed to be also high. In addition, owing to the high ion density of DC arc plasma, the ion flux bombarding the substrate is high. Bias current in the present method is of the order of 100–200 mA/cm^2, which is over 100 times larger than that of usual ion-assisted methods. According to the momentum transfer theory [2,27], the energy of each particle necessary to form cBN decreases with increasing ion flux. The optimum bias voltage is -85 V in our experiments, but the effective voltage must be much lower at a high gas pressure of 50 torr, owing to the frequent collisions during the acceleration in the plasma sheath. Berns and Cappelli [13] calculated the ion energy distribution for their expanding nitrogen/argon plasma and roughly estimated the average ion energy as 18 eV, when a -75-V substrate bias was applied, while the pressure at the substrate surface was estimated to be 5 torr at the chamber pressure of 0.1–1 torr. The chamber pressure of our experiments was 50 torr, which is approximately two orders of magnitude higher than that of theirs. Then the average ion energy must be much lower than 18 eV.

Using the growth rate of 0.3 μm/min and the bias current of 100 mA/cm^2 and assuming the bombarding energy of Ar ions as 10 eV, we estimated the P_{Tot}/a value to be approximately 400 (emu.eV)$^{1/2}$, which is higher than the critical value of 200 evaluated for cBN formation [2,27]. If we use an arriving rate of boron instead of the depositing one, assuming the concentration of boron in the gas phase is equal to that fed and the pressure and the gas temperature at the substrate surface are 100 torr and 2000 K, respectively, the P_{Tot}/a value becomes approximately 40, which means only 10% of impinging boron atoms are deposited. Since we can consider that BF_3 is almost completely decomposed to BF_x ($x = 2,1,0$) or converted to the BHF_2 form the equilibrium calculation of the gas phase in the thermal plasma [28], the formation of cBN at such a low P_{Tot}/a can be attributed to the low deposition probability of such species or the high reactivity of fluorine with the surface; in other words, the etching effect of fluorine. Furthermore, because the growth rate of cBN at early stages (ca. 3 μm/10 min) is higher than that of the amorphous/hBN interlayers (0.15 μm/1–3 min), we can say that preferential etching for sp^2 BN of fluorine is working. Although the growth rate of cBN of our method is the highest ever reported, it is still more than one order of magnitude lower than the value for diamond growth by DC jet CVD. The selectivity of fluorine to cBN and hBN seems to be lower than that of atomic hydrogen to graphitic carbon and diamond.

The atomic processes of the effect of fluorine is not yet clear. Highly reactive fluorine atoms and molecules will react with cBN as well as hBN to form B–F and N–F bonds, stabilizing sp^3 bonds on the surface or etch them back to the gas phase. Preferential etching of hBN by fluorine was demonstrated by Kalss et al. [29]. Furthermore, fluorine was found to be effective in stabilizing the B (111) surface of cBN by theoretical calculation [30]. These preferential etching and surface stabilizing effects of fluorine correspond to those of atomic hydrogen in diamond CVD. However, it is also calculated that the stabilized B (111) surface does not react with nitrogen-containing species, preventing the growth of cBN [30]. Atomic hydrogen is considered to form an active site on a diamond surface by the hydrogen abstraction reaction. Such a reaction by a fluorine atom on fluorinated BN surfaces is probably energetically unfavorable. Abstraction reactions by an atomic hydrogen seems unfavorable too, as calculated for surface fluorine on B (111) [30]. Therefore, substrate bias must be working to activate such a stable cBN surface bonded with fluorine, if such a surface exists under our deposition conditions. Substrate bias can be supposed to contribute also to activate chemisorbed species and arriving ions (N_2^+, BF_x^+, etc.) themselves on the growing surface. Sub-plantation, sputtering, and stress accumulation mechanisms have been proposed for cBN formation [23,24]. For these mechanisms, a kinetic energy of ions much higher than the average value estimated above is necessary. Although it is necessary to consider the effects of ions at the high-energy tail of an ion energy distribution function, low stress in our films suggests surface chemical effects by the bias mentioned above are predominating. Although the interlayer structure of Si/amorphous BN/hortBN/cBN is present in our films also, the larger thickness of the intermediate layers, loose preferred orientation of the hBN layers, and the low density of nucleation sites make it unclear whether the cBN nucleation sites are similar to those in the ion-assisted methods used so far or at some arbitrary spots.

References

[1] K. Inagawa, K. Watanabe, H. Ohsone, K. Saitoh, A. Itoh, J. Vac. Sci. Technol. A 5 (1987) 2696.
[2] D.J. Kester, R. Messier, J. Appl. Phys. 72 (1992) 504.
[3] T.A. Friedmann, P.R. Mirkarimi, D.L. Meddlin et al., J. Appl. Phys. 76 (1994) 3088.
[4] M. Lu, A. Bousetta, R. Sukach et al., Appl. Phys. Lett. 64 (1994) 1514.
[5] H. Hofsäss, C. Ronning, U. Griesmeier, M. Gross, S. Reinke, M. Kuhr, Appl. Phys. Lett. 67 (1995) 46.
[6] O. Tsuda, Y. Yamada, T. Fujii, T. Yoshida, J. Vac. Sci. Technol. A 13 (1995) 2843.
[7] D. Litvinov, R. Clarke, Appl. Phys. Lett. 71 (1997) 1969.
[8] M. Okamoto, Y. Utsumi, Y. Osaka, Plasma Sources Sci. Technol. 2 (1993) 1.
[9] A. Weber, U. Bringmann, R. Nikulski, C.P. Klages, Surf. Coat. Technol. 2 (1993) 201.
[10] W. Dworschak, K. Jung, H. Ehrhardt, Diamond Relat. Mater. 3 (1994) 337.
[11] T. Ichiki, T. Momose, T. Yoshida, Appl. Phys. Lett. 75 (1994) 1330.
[12] M. Kuhr, S. Reinke, W. Kulisch, Surf. Coat. Technol. 74–75 (1995) 806.
[13] D.H. Berns, M.A. Cappelli, J. Mater. Res. 12 (1997) 2014.
[14] D.R. McKenzie, W.D. McFall, W.G. Sainty, C.A. Davis, R.E. Collins, Diamond Relat. Mater. 2 (1993) 970.
[15] M. Murakawa, S. Watanabe, Surf. Coat. Technol. 43 (1990) 1.
[16] W. Donner, H. Dosch, S. Ulrich, H. Ehrhardt, D. Abernathy, Appl. Phys. Lett. 73 (1998) 777.
[17] P. Widmayer, P. Ziemann, S. Ulrich, H. Ehrhardt, Diamond Relat. Mater. 6 (1997) 621.
[18] S. Matsumoto, W.J. Zhang, Jpn. J. Appl. Phys. 39 (2000) L442.
[19] H. Kohzuki, M. Motoyama, J. Japan Inst. Metals 56 (1992) 565 in Japanese..
[20] V.L. Solozhenko, V.V. Chernyshev, G.V. Fetisov, V.B. Rybakov, I.A. Petrusha, J. Phys. Chem. Solids 51 (1990) 1011.
[21] W.J. Zhang, S. Matsumoto, Presented in 7th Int. Conf. New Diamond Sci. Tecnol., Hong Kong (2000).
[22] W.J. Zhang, S. Matsumoto, Phys. Rev. B. 63 (2001) 073201.
[23] T. Yoshida, Diamond Relat. Mater. 5 (1996) 501 (see references therein).
[24] P.R. Mirkarimi, K.F. McCarty, D.L. Meddlin, Mater. Sci. Eng. R21 (1997) 47 (see references therein).

[25] S. Matsumoto, I. Hosoya, Y. Manabe, Y. Hibino, Pure Appl. Chem. 64 (1992) 751.
[26] W.J. Zhang, S. Matsumoto, unpublished data.
[27] P.R. Mirkarimi, K.F. McCarty, D.L. Meddlin et al., J. Mater. Res. 9 (1994) 2925.
[28] S. Matsumoto, N. Nishida, K. Akashi, K. Sugai, J. Mater. Sci. 31 (1996) 713.
[29] W. Kalss, R. Haubner, B. Lux, Diamond Relat. Mater. 7 (1998) 369.
[30] K. Larsson, J.-O. Carlsson, J. Phys. Chem. B 103 (1999) 6533.